Title: *apterous A* specifies dorsal wing patterns and sexual traits in butterflies

Authors: Anupama Prakash[1*] and Antónia Monteiro[1,2*]

Affiliations:

[1] Department of Biological Sciences, National University of Singapore, Singapore.

[2] Yale-NUS College, Singapore.

*Correspondence to: anupama@u.nus.edu or antonia.monteiro@nus.edu.sg

Abstract: Butterflies have evolved different color patterns on their dorsal and ventral wing surfaces to serve different signaling functions, yet the developmental mechanisms controlling surface-specific patterning are still unknown. Here, we mutate both copies of the transcription factor *apterous* in *Bicyclus anynana* butterflies using CRISPR/Cas9 and show that *apterous A* functions both as a repressor and modifier of ventral wing color patterns, as well as a promoter of dorsal sexual ornaments in males. We propose that the surface-specific diversification of wing patterns in butterflies proceeded via the co-option of *apterous A* into various gene regulatory networks involved in the differentiation of discrete wing traits. Further, interactions between *apterous* and sex-specific factors such as *doublesex* may have contributed to the origin of sexually dimorphic surface-specific patterns. Finally, we discuss the evolution of eyespot pattern diversity in the family Nymphalidae within the context of developmental constraints due to *apterous* regulation.

Main Text:

Butterflies are a group of organisms well known for their diverse and colorful wing patterns. Due to the dual role these patterns play in survival and mate selection, many butterflies have evolved a signal partitioning strategy where color patterns appearing on the hidden dorsal surfaces generally function in sexual signaling, whereas patterns on the exposed ventral surfaces most commonly serve to ward off predators (*1*, *2*) [Fig 1A]. While the molecular and developmental basis of individual pattern element differentiation, such as eyespots or transverse bands, has been previously studied (*3*, *4*), the molecular basis of dorsal and ventral surface-specific color pattern development remains unknown. Elucidating this process will help us understand the mechanism of diversification and specialization of wing patterns within the butterfly lineage.

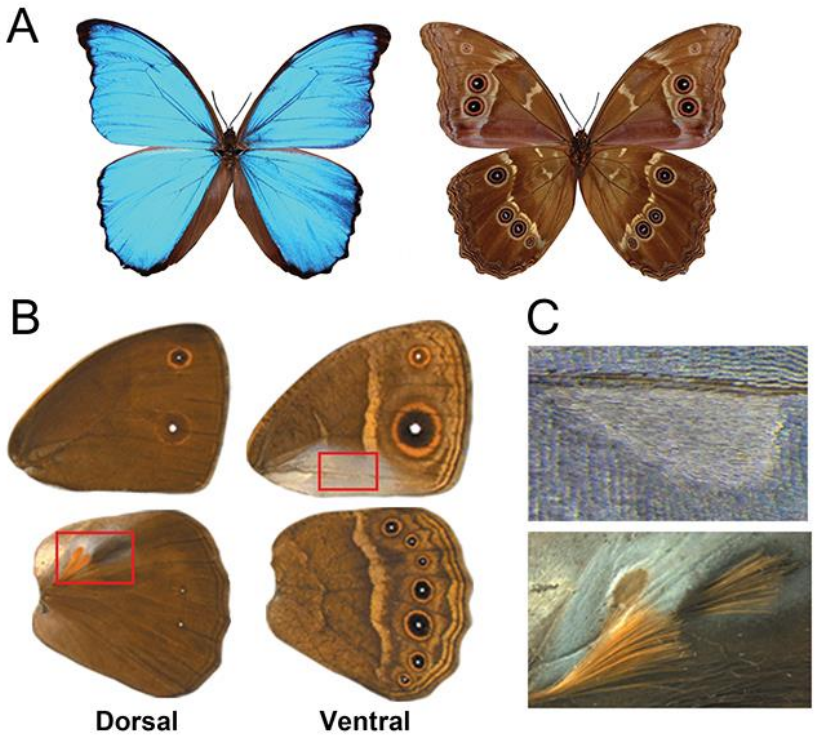

Figure 1: Dorsal-Ventral surface-specific variation in butterflies A) Dorsal (left) and ventral (right) surfaces of *Morpho menelaus* illustrating striking variation in color and patterns between surfaces. B) Dorsal and ventral surfaces of a male *Bicyclus anynana*. The regions boxed in red are expanded in C. C) Top: Male-specific forewing ventral androconia with a characteristic teardrop shape surrounded by silver scales. This is absent from the corresponding dorsal forewing surface which is instead completely covered with brown scales. Bottom: Male-specific hindwing dorsal androconia, also surrounded by silver scales, along with two patches of hair-pencils. These traits are absent from the ventral hindwing.

We hypothesized that the transcription factor *apterous (ap)*, a gene expressed in the dorsal wing surfaces of flies (*5*), might be implicated in differentiating dorsal from ventral wing patterns in butterflies. In insects, however, this gene is often present in two copies, *apA* and *apB*, that don't necessarily share the same expression patterns, and flies are unusual for having lost one of these copies. In the beetle *Tribolium castaneum*, *apA* is expressed on the dorsal surface whereas *apB* is expressed on both surfaces (*6*). In the butterfly *Junonia coenia, apA* is expressed on the dorsal surface of larval wings (*7*) but, the expression of *apB* and the role of either *apA* or *apB* in wing development and patterning is not known for this or any butterfly species.

To further investigate *ap* expression in butterflies, we cloned both *ap* homologs from the African squinting bush brown *Bicyclus anynana* [Fig 1B, C], and used *in situ* hybridization to localize *apA* and *apB* mRNA in developing larval and pupal wing discs. Both homologs of a*p* were localized to the dorsal surfaces of the wings [Fig 2D, S1B]. In the last larval instar wing discs, *apA* was expressed uniformly on the wing surface but absent in future dorsal eyespot centers [Fig2A]. In larval wing discs of the *B. anynana* "Spotty" mutant, which develops two additional dorsal eyespots, *apA* was absent in the additional centers [Fig 2C]. Furthermore, pupal wing expression of both *apA* and *apB* was up-regulated in dorsal male-specific cells that give rise to long and thin modified scales, the hair-pencils, used for dispersing pheromones during courtship [Fig 2B, S1A]. This pattern of expression was not seen in developing female pupal wings, which lack hair-pencils [Fig S1A].

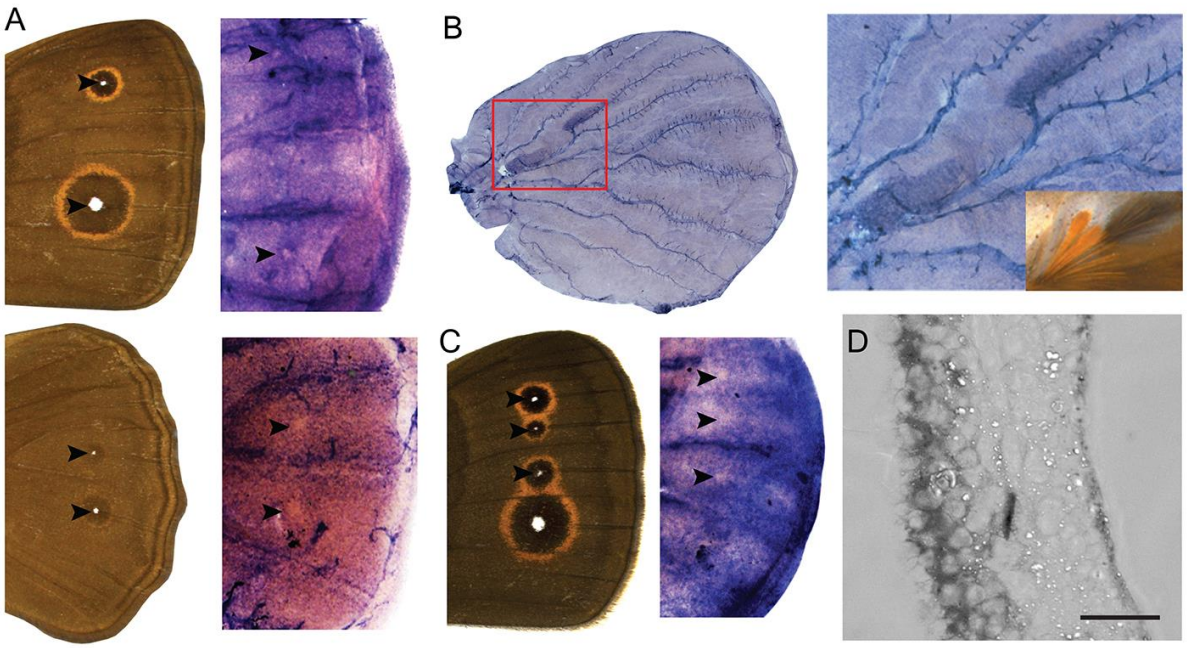

Figure 2: *apA* mRNA localization in developing wing discs of *Bicyclus anynana* A) *apA* expression is uniform across the epidermis but absent in future dorsal eyespot centers of forewings (top) and hindwings (bottom). B) Male wings (28 hours after pupation) showing *apA* mRNA localization. The boxed area is expanded to the right highlighting up-regulated *apA* expression in the hair-pencil regions. Inset shows the hair-pencils in adult male *B. anynana*. C) *apA* expression is absent in the two additional eyespot centers of forewings in the *B. anynana* "Spotty" mutant. D) Cross-sectional view of a developing wing disc showing dorsal-specific *apA* expression. Scale bar is 20µm.

To functionally test the role of *ap*, we used the CRISPR/Cas9 system to disrupt the homeodomain and LIM domain of *apA* [Fig 3A] and the LIM domain of *apB* [Fig S2A] [Table S2]. A range of mosaic phenotypes were observed in both types of *apA* mutant individuals [Fig 3B-F]. A few of these lacked wings, whose absence was visible upon pupation [Fig 3F], and some adults had mosaic patches of ventral-like scales appearing on the dorsal surface [Fig 3E]. In other mutants, the sex pheromone producing organ, the androconial organ, of the ventral forewing appeared on the dorsal surface in males with its associated silver scales [Fig 3B,C]. Males also had modified hair-pencils with loss of characteristic ultrastructure and coloration and absence of silver scales associated with the dorsal androconial organ of the hindwing [Fig3B]. In addition, in some males and females, extreme mutant individuals showed improper wing hinge formation, the appearance of the ventral white band on the dorsal surface [Fig 3B], and in one case, all seven eyespots on the dorsal hindwing [Fig 3B], a surface that normally exhibits, on average, zero to one eyespot in males and one to two eyespots in females. *apA* clones also led to an enlarged outer perimeter to the gold ring in dorsal hindwing and forewing eyespots [Fig 3D]. CRISPR/Cas9 disruption effects on the target sequence were verified in a few individuals, which showed the presence of deletions in the targeted regions [Fig 3A].

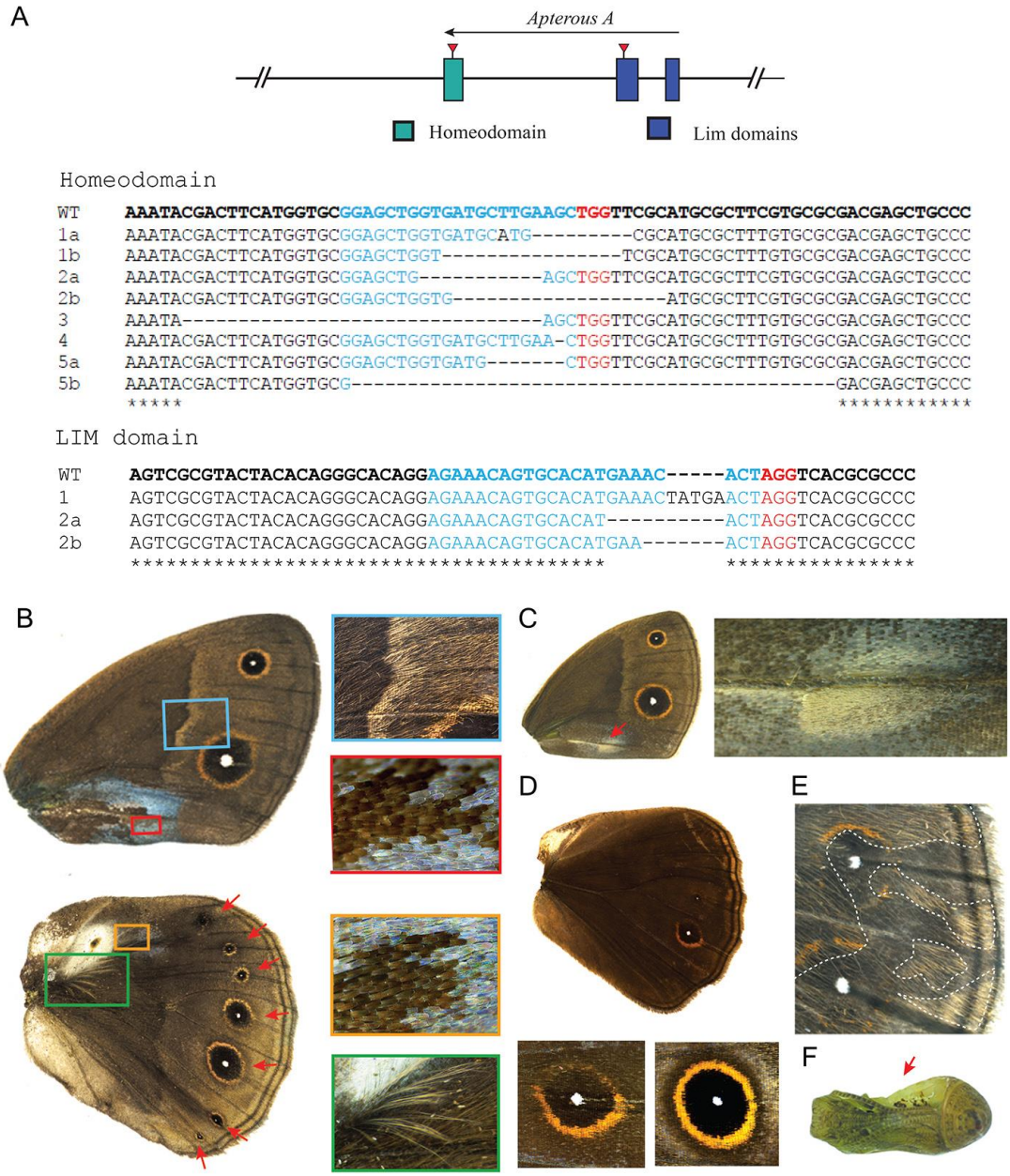

93

94 **Figure 3: CRISPR/Cas9 mosaic wing pattern phenotypes of *apA* knockdown** A) Top:

95 Regions of the *apA* gene in *B. anynana* targeted using the CRISPR/Cas9 system. Bottom:

96 Sequences of the homeodomain and LIM domain regions of mutant individuals compared with

97 the wildtype sequence in bold. Blue is the region targeted and the PAM sequence is in red.

98 Deletions are indicated with '-'. B) The dorsal forewing and hindwing of a mutant male

99 highlighting some of the ventral-like phenotypes and defects. C) *apA* knockdown phenotype with

the ventral teardrop shape androconial organ appearing on the dorsal surface (red arrow). D) A dorsal hindwing of a mutant with the width of the gold ring (bottom left) resembling that of corresponding ventral eyespot (bottom right). E) Mosaic phenotype seen on the dorsal surface with a greater density of ventral-like light colored scales. Clones are indicated with a dashed white line. F) Pupa with wings missing from one side (red arrow).

No striking transformations of dorsal to ventral identity were observed in *apB* mutants. Some of the *apB* knockout phenotypes included wing hinge defects, a clone of ventral-like scales on the dorsal surface [Fig S2E], affected hair pencils [Fig S2D], a missing hindwing in one case, improperly developed wings [Fig S2C] and notched margin development [Fig S2B]. Sequencing showed the presence of mutations in the targeted region [Fig S2A].

Knockdown of *apA* in a variety of insects from different lineages indicates that *apA* is necessary for wing growth and development and its function in this process seems to be highly conserved (*5*, *6*, *8*). However, our experiments, in agreement with others, also indicate a varying degree of co-option of this transcription factor into late wing development processes such as wing patterning and exoskeletalization. In *T.castaneum*, knockdown of *apA* and *apB* individually shows almost no phenotypic effects while their simultaneous knockdown leads to more dramatic phenotypes such as elytral exoskeletalization defects, depending on the developmental stage. Therefore, both *apA* and *apB* in beetles are important for wing developmental processes (*6*). In *B. anynana*, both *ap* copies appear to function in margin specification and overall wing development but only *apA* appears to have a dominant role in the control of dorsal-surface specific wing patterning.

Interestingly, our work shows that *apA* has multiple different, often antagonistic functions in surface- and sex-specific development between the fore- and hindwings. For example, *apA* acts as a repressor of male androconial organs and silver scale development in forewings, while it promotes hair-pencil formation and silver scale development on the dorsal hindwings of males [Fig 4A]. These effects point to the likely interaction between *apA* and other factors such as sex-

specific (*doublesex*) or wing-specific (*Ultrabithorax*) factors that together can specify sex- and surface-specific pattern development. We previously showed that *Ultrabithorax* (*Ubx)* is expressed in the hindwings but not forewings of *B. anynana* (*9*). To verify whether genes from the sex determination pathway were present in androconial organs of *B. anynana* we localized the expression of *doublesex (dsx)* in both male and female pupal wings using *in situ* hybridization. We found that *dsx* is highly expressed in male androconial organs and hair-pencils, but not in corresponding locations on female wings [Fig S1D]. These data support a likely combinatorial function reminiscent of the interactions between the hox gene *Scr* and *dsx* in the determination of the male-specific sex combs in the legs of *D. melanogaster* (*10*). The presence or absence of *Ubx*, type of *dsx* splice variant and *apA* may be sufficient to give each sex and wing surface a unique identity. Given the fact that the proteins of the LIM-homeodomain subfamily, to which *ap* belongs, are unique in their ability to bind other proteins via their LIM domain (*11*), their involvement in such a large range of developmental processes, as repressors and activators, is likely.

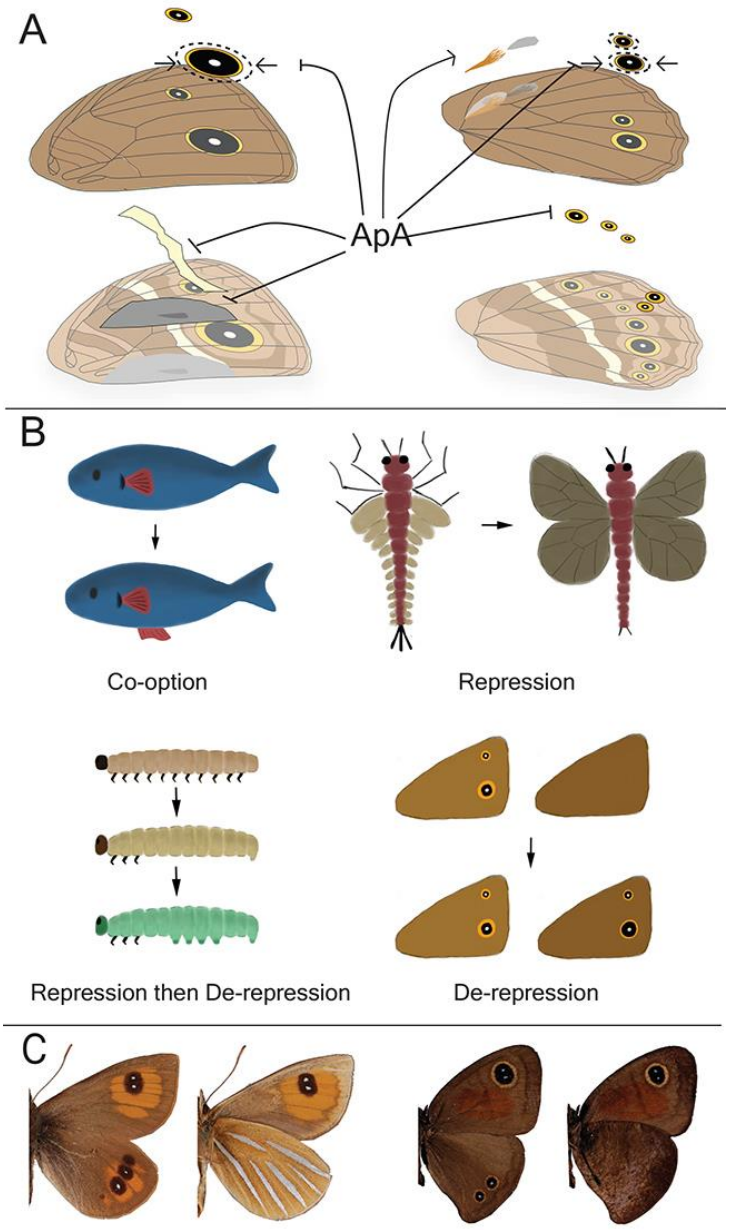

Figure 4: The role of *apterous* in surface-specific wing patterning in *B. anynana* and evolution of serial homologs in butterflies. A) A schematic of the different functions of *apA* on the dorsal surface of *B. anynana*. *apA* acts as a repressor of ventral traits such as the white transversal band, forewing androconia, hindwing eyespots, and the outer perimeter of the gold ring, and acts as an activator of hindwing hair-pencils and silver scales. B) Different modes of serial homolog evolution involving the co-option of a (fin) gene network to a novel body

location (*23*), repression of the ancestrally repeated (wing) network in a subset of body segments (modified from (*24*)), repression followed by de-repression of the (limb) network in certain body segments (*20*), and de-repression of a never expressed (eyespot) network on a novel body location. C) *Argyrophenga antipodium* (left) and *Cassionympha cassius* (right) males with dorsal eyespots lacking ventral counterparts. Dorsal is to the left for each species.

158 Mutations in *apA* point to this gene functioning as a dorsal surface selector in *Bicyclus*
159 butterflies. Selector genes comprise a small set of developmental genes that are critical for
160 specifying cell, tissue, segment, or organ identities in organisms (*12*).The wing selector hox gene
161 *Ubx* allows hindwings to have a different identity from forewings. For example, the restricted
162 expression of *Ubx* in hindwings of most insects examined so far, is required for membranous
163 wing formation in beetles and bugs (*13*), haltere formation in flies (*14*) and hindwing specific
164 color patterns in butterflies (*15*). When *Ubx* is mutated, in all the examples described above,
165 hindwings acquire the identity of forewings. In *B. anynana*, *apA* functions in similar ways along
166 the dorsal-ventral axis of each wing – mutations in this gene make dorsal wing surfaces acquire a
167 ventral identity. This type of homeotic mutation was also observed in a limited way, in bristles
168 along the margin of the wings of *D. melanogaster,* where *ap* mutant clones developed bristles
169 with a ventral identity (*16*). *B. anynana*, however, appears to have made inordinate use of *apA*
170 for surface-specific color patterning and sexual trait development across the entire wing.
171
172 Further, this work highlights the possible role of apA in the development and evolution of serial
173 homologs such as eyespots in butterflies of the family Nymphalidae. The appearance of
174 additional eyespots on the dorsal surface of hindwings in *apA* knockdown mutants, and the
175 absence of *apA* mRNA at the precise position where a few dorsal eyespots develop in both fore-
176 and hindwings at the stage of eyespot center differentiation, implicates *apA* as a repressor of
177 eyespot development in *B. anynana.* The additional gaps in *apA* expression observed in Spotty
178 mutants further suggests that genetic mechanisms of eyespot number evolution on the dorsal
179 surface proceeded via local repression of *apA.*
180

We propose that the ancestral presence of a repressor (*apA*) of a gene regulatory network in a specific body location, followed by repression of the repressor represents a novel mode of serial homolog diversification [Fig 4B]. Broad comparative work across 400 genera of butterflies indicated that eyespots originated around 90 MYA within Nymphalidae on the ventral hindwing surface, and appeared ~40MY later on the dorsal surfaces (*17–19*). We propose that the original ventral restriction of eyespots was due to the ancestral presence of *apA* on dorsal wing surfaces, and that eyespots' later appearance on these surfaces was due to local *apA* repression. This mode of serial homolog diversification is similar but also distinct from the mechanism previously proposed to lead to the re-appearance of abdominal appendages in lepidopteran larvae - via local repression of the limb repressor hox protein, *Abdominal-A* (*Abd-A*) (*20*, *21*). In contrast to eyespots, when arthropod appendages first originated they were likely present in every segment of the body (*22*). Limbs were later repressed in abdominal segments, and finally they were de-repressed in some of these segments in some insect lineages (*20*). So, while the last steps of abdominal appendage and eyespot number diversification are similar (de-repression of a repressed limb/eyespot network), the early stages are different.

The comparative work also showed that the origin of dorsal eyespots was dependent on the presence of corresponding ventral eyespots in ancestral lineages (*19*). This implies that the extant diversity of eyespot patterns is biased/limited due to developmental constraints imposed by *apA*. Interestingly, while ~99% of the species in our database display such constraints i.e dorsal eyespots always having ventral counterparts, a few butterflies display dorsal eyespots that lack ventral counterparts [Fig 4C]. The molecular basis for these rare patterns remains to be explored.

In summary, we uncover a key transcription factor that due to its restricted expression on dorsal wing surfaces may have allowed butterflies to develop and evolve their strikingly different dorsal and ventral wing patterns under natural and sexual selection. Future comparative work across species is necessary to further test this hypothesis.

References and Notes:

1. D. J. Kemp, Female butterflies prefer males bearing bright iridescent ornamentation. *Proc. Biol. Sci.* **274**, 1043–1047 (2007).
2. K. L. Prudic, A. M. Stoehr, B. R. Wasik, A. Monteiro, Eyespots deflect predator attack increasing fitness and promoting the evolution of phenotypic plasticity. *Proc. Biol. Sci.* **282**, 20141531 (2015).
3. A. Monteiro, Origin, Development, and Evolution of Butterfly Eyespots. *Annu. Rev. Entomol.* **60**, 253–271 (2015).
4. A. Martin, R. D. Reed, Wingless and aristaless2 define a developmental ground plan for moth and butterfly wing pattern evolution. *Mol. Biol. Evol.* **27**, 2864–2878 (2010).
5. B. Cohen, M. E. McGuffin, C. Pfeifle, D. Segal, S. M. Cohen, Apterous, a gene required for imaginal disc development in Drosophila encodes a member of the LIM family of developmental regulatory proteins. *Genes Dev.* **6**, 715–729 (1992).
6. Y. Tomoyasu, Y. Arakane, K. J. Kramer, R. E. Denell, Repeated Co-options of Exoskeleton Formation during Wing-to-Elytron Evolution in Beetles. *Curr. Biol.* **19**, 2057–2065 (2009).
7. S. B. Carroll *et al.*, Pattern Formation and Eyespot Determination in Butterfly Wings. **265**, 109–113 (1994).

8. F. Z. Liu *et al.*, Apterous A modulates wing size, bristle formation and patterning in Nilaparvata lugens. *Sci. Rep.* **5**, 1–12 (2015).

9. X. Tong, S. Hrycaj, O. Podlaha, A. Popadic, A. Monteiro, Over-expression of Ultrabithorax alters embryonic body plan and wing patterns in the butter fl y Bicyclus anynana. *Dev. Biol.* **394**, 357–366 (2014).

10. K. Tanaka, O. Barmina, L. E. Sanders, M. N. Arbeitman, A. Kopp, Evolution of sex-specific traits through changes in HOX-dependent doublesex expression. *PLoS Biol.* **9**, e1001131 (2011).

11. O. Hobert, H. Westphal, Functions of LIM- homeobox genes. *Trends Genet.* **16** (2000).

12. R. Mann, S. Carroll, Molecular mechanisms of selector gene function and evolution. *Curr. Opin. Genet. Dev.* (2002).

13. M. Whitney, Y. Tomoyasu, S. R. Wheeler, R. E. Denell, Ultrabithorax is required for membranous wing identity in the beetle Tribolium castaneum, 643–647 (2005).

14. E. B. Lewis, Genes and Developmental Pathways. *Am Zool.* **3**, 33–56 (1963).

15. S. D. Weatherbee *et al.*, Ultrabithorax function in butterfly wings and the evolution of insect wing patterns. *Curr. Biol.* **9**, 109–115 (1999).

16. F. J. Diaz-Benjumea, S. M. Cohen, Interaction between dorsal and ventral cells in the imaginal disc directs wing development in Drosophila. *Cell*. **75**, 741–752 (1993).

17. J. C. Oliver, X. Tong, L. F. Gall, W. H. Piel, A Single Origin for Nymphalid Butterfly Eyespots Followed by Widespread Loss of Associated Gene Expression. **8** (2012), doi:10.1371/journal.pgen.1002893.

18. J. C. Oliver, J. M. Beaulieu, L. F. Gall, W. H. Piel, A. Monteiro, Nymphalid eyespot serial homologues originate as a few individualized modules. *Proc. R. Soc. B Biol. Sci.* **281**,

20133262–20133262 (2014).

19. S. R. Schachat, J. C. Oliver, A. Monteiro, Nymphalid eyespots are co-opted to novel wing locations following a similar pattern in independent lineages. *BMC Evol. Biol.* **15**, 20 (2015).

20. R. Warren, L. Nagy, J. Selegue, J. Gates, S. Carroll, Evolution of Homeotic Gene regulation and function in flies and butterflies (1994).

21. Y. Suzuki, M. Palopoli, Evolution of insect abdominal appendages : Are prolegs homologous or convergent traits ? *Dev. Genes Evol.* **211**, 486–492 (2001).

22. N. Shubin, C. Tabin, S. Carroll, Fossils, genes and the evolution of animal limbs. *Nature*. **388**, 639–48 (1997).

23. I. Ruvinsky, J. J. Gibson-Brown, Genetic and developmental bases of serial homology in vertebrate limb evolution. *Development*. **127**, 5233–5244 (2000).

24. S. B. Carroll, S. D. Weatherbee, J. a Langeland, Homeotic genes and the regulation and evolution of insect wing number. *Nature*. **375** (1995), pp. 58–61.

25. I. C. Conceicao, A. D. Long, J. D. Gruber, P. Beldade, Genomic sequence around butterfly wing development genes: Annotation and comparative analysis. *PLoS One*. **6** (2011), doi:10.1371/journal.pone.0023778.

26. A. R. W. Nowell, B. Elsworth, V. Oostra, B. J. Zwaan, A high-coverage draft genome of the mycalesine butterfly *Bicyclus anynana*. *GIGA Sci.* (in press).

27. D. Ramos, A. Monteiro, In situ protocol for butterfly pupal wings using riboprobes. *J. Vis. Exp.*, 208 (2007).

28. A. R. Bassett, C. Tibbit, C. P. Ponting, J. L. Liu, Highly Efficient Targeted Mutagenesis of Drosophila with the CRISPR/Cas9 System. *Cell Rep.* **4**, 220–228 (2013).

Acknowledgments: We thank Arjen van't Hof and Luqman Aslam for their help in retrieving sequence information from the *B. anynana* genome, Mainak Das Gupta for his help in the *in situ* hybridization protocols and Monteiro lab members for their support. This work was funded by Ministry of Education, Singapore grant R-154-000-602-112, the National University of Singapore grant R-154-000-587-133, and by the Department of Biological Sciences, NUS.

Supplementary Materials:

Materials and Methods

Animals

Bicyclus anynana butterflies were reared in a temperature controlled room at 27°C with a 12:12 hour light:dark cycle and 65% humidity. The larvae were fed on corn plants while the adults were fed on banana.

Cloning and probe synthesis

apA sequence was obtained from (*25*) and *apB* and *dsx* sequences were identified from the *B.anynana* genome (*26*).The sequences were amplified with primers specified in Table S1, sequenced and then cloned into a PGEM-T Easy vector (Promega). Sense and anti-sense digoxigenin-labelled (DIG) riboprobes were synthesized *in vitro* using T7 and SP6 polymerases (Roche) and purified by ethanol precipitation. The product was hydrolysed to ~150bp using carbonate buffer at 60°C for 40-50 minutes followed by ethanol precipitation and resuspension in 1:1 volume of DEPC treated water:formamide.

In-situ hybridization

The protocol was modified slightly from (*27*). Briefly, larval or pupal wings were dissected from the last instar caterpillars or around 24-28 hrs after pupation respectively in PBS and transferred to glass well plates containing PBST (PBS+0.1% Tween20) at room temperature. The PBST was then immediately removed and the tissues fixed in 5% formaldehyde for 45 (larval) or 60 min (pupal) on ice, followed by 5 washes with cold PBST. The tissues were then incubated with 25µg/ml proteinase K in cold PBST for 3 (larval) or 5 minutes (pupal), washed twice with 2mg/ml glycine in cold PBST, 5 washes with cold PBST and gradually transferred to a prehybridization buffer (5X Saline sodium citrate pH 4.5, 50% formamide, 0.1% Tween20 and 100µg/ml denatured salmon sperm DNA). A post-fixation step with 5% formaldehyde was done only for larval wings followed by removal of peripodial membrane on ice (just for larval wings). The wings were incubated in prehybridization buffer at 60-65°C for 1 hour and then in hybridization buffer (prehybridization buffer with 1g/L glycine and 70 to 140 ng/ml riboprobe) for 24 hours, followed by 6 to 10 washes in prehybridization buffer at 60-65°C. The tissues were then gradually transferred back to PBST at room temperature, washed 5 times in PBST and blocked overnight at 4°C (PBST+1% BSA). The DIG-labelled probes were then detected by incubating the tissues with 1:3000 Anti-DIG Alkaline Phosphatase (Roche) in block buffer for two hours, washed 5 times with block buffer, incubated in alkaline phosphatase buffer (100mM Tris pH 9.5, 100mM NaCl, 5mM $MgCl_2$, 0.1% Tween) and finally stained with NBT/BCIP (Promega) solution at room temperature till colour developed. The reaction was stopped by washing in 2mM EDTA in PBST and again with PBST. The sections were either mounted on slides with ImmunoHistoMount medium (Abcam) or post-fixed with 5% formaldehyde before wax embedding and sectioning (Advanced Molecular Pathology Lab, IMCB, Singapore).

Preparation of Cas9 mRNA and guide RNA

pT3TS-nCas9n was a gift from Wenbiao Chen (Addgene plasmid #46757). The plasmid was linearized with XbaI digestion and purified using a GeneJET PCR Purification Kit (Thermo Scientific). Cas9 mRNA was obtained by in vitro transcription using the mMESSAGE

mMACHINE T3 kit (Ambion), tailed using the Poly(A) Tailing Kit (Ambion) and purified by lithium chloride precipitation. The guide RNA templates were prepared using a PCR based method according to (*28*). The candidate targets were manually designed by searching for a $GGN_{18}NGG$ sequence on the sense or anti-sense strand of *apA* and *apB*, preferably targeting the LIM and homeobox domains of the transcription factor (Table S1). They were blasted against the *B. anynana* genome on LepBase.org to check for off-target effects. The template DNA sequence was used to perform an *in vitro* transcription using T7 RNA polymerase (Roche) at 37°C overnight, purified by ethanol precipitation and re-suspended in DEPC treated water.

Microinjections

Eggs were collected on corn leaves within one to two hours of egg laying and were arranged on thin strips of double-sided tape on a petri dish. Cas9 mRNA and guide RNAs were mixed along with green food dye (1:80) (Table S2) and injected into the eggs with a Borosil glass capillary (World Precision Instruments, 1B100F-3) using a Picospritzer II (Parker Hannifin). A piece of wet cotton was placed in the petri dish and the eggs were allowed to develop in an incubator at 27°C and high (~80%) humidity. Hatched caterpillars were placed on young corn plants using a brush. Adults that emerged were scored for their phenotypes (Table S2).

Sequencing and genotyping mutants

Genomic DNA was extracted from leg tissues of mutant individuals using the E.Z.N.A Tissue DNA Kit (Omega Bio-tek). The region surrounding the target sequence was amplified by PCR, purified by ethanol precipitation, and used to check for presence of mutations using the T7 endonuclease I (T7EI) assay. Sequences from individuals with disruptions at the targeted regions were cloned into a PGEM-T Easy vector (Promega) and sequenced.

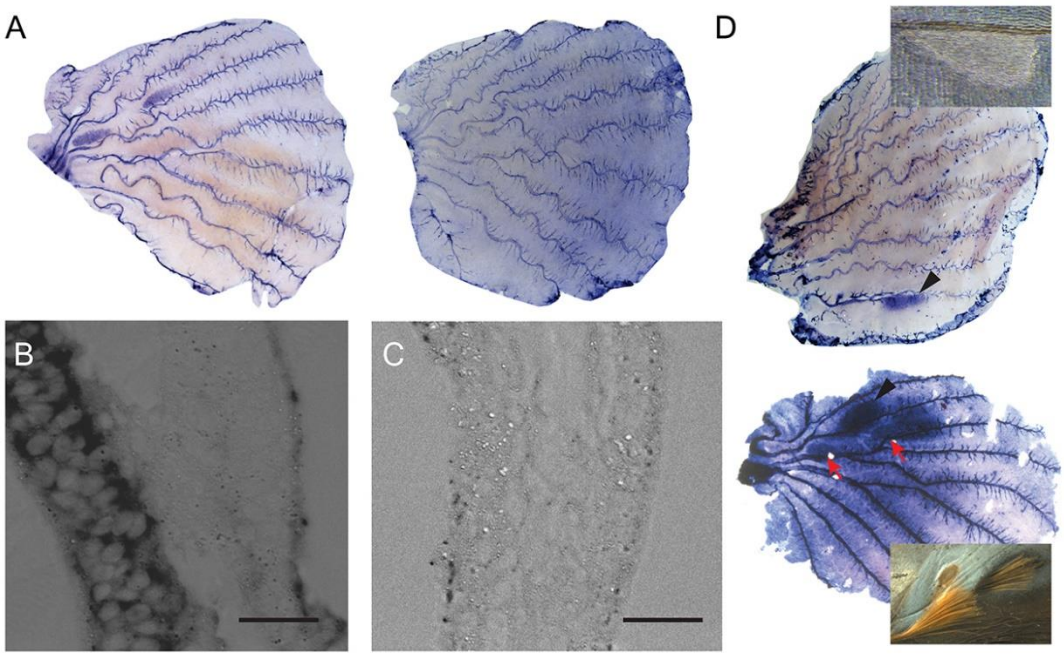

.

Figure S1: ***apB* and *dsx* mRNA localization in developing wing discs of *Bicyclus anynana*** A) Male (left) and female (right) hindwing discs (28 hours after pupation) showing *apB* mRNA localization. Up-regulated *apB* expression in the hair-pencil regions is seen only in male wings. B) Cross-sectional view of a developing wing disc showing dorsal-specific *apB* expression. C) Cross-sectional view of a developing wing disc stained with *apB* sense probe as control. Scale bar for B and C is 20µm. D) *dsx* mRNA localization in a male forewing and hindwing (~30 hours after pupation) with upregulation in future androconial (arrowheads) and hair-pencil regions (red arrows). Insets show the androconia and hair-pencils in adults.

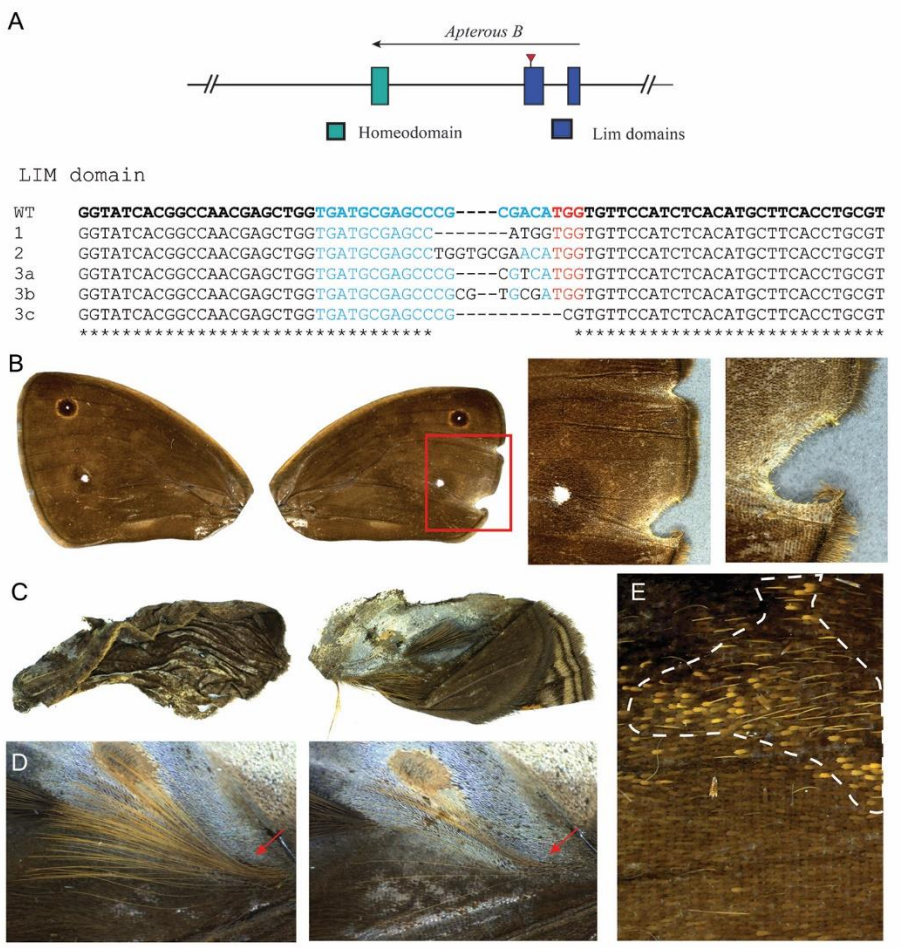

Figure S2: **CRISPR/Cas9 mosaic wing pattern phenotypes of *apB* knockout** A) Top: Region of the *apB* gene in *B.anynana* targeted using the CRISPR/Cas9 system Bottom: Sequences of the LIM domain region of mutant individuals compared with the wildtype sequence in bold. Blue is the region targeted and the PAM sequence is in red. Deletions are indicated with '-'. B) The forewings of a mutant individual showing differences in shape and marginal defects of the right wing as compared to the left. The boxed area is expanded to the right. C) *apB* knockout mosaic phenotype with overall wing development affected. D) A mutant with reduced number of hair-pencils (right) as compared to a control (left). Red arrows indicate the base of the hair-pencils. E) Mosaic phenotype seen on the dorsal surface with a greater density of ventral-like light colored scales. The clone is indicated with a dashed white line.

Table S1: List of primers and guide RNA sequences used in this study

Gene	Primer Name	Primer Sequence
Apterous A (*ApA*)	AM 31 AM 32	Forward 5' CGGGAGGCCTGTCTTCTGGC 3' Reverse 5' CGTCGGAGCTGGTGATGAGGG 3'
Apterous B (*ApB*)	AM 136 AM 137	Forward 5' CGAACAGTTGAATGCGTATTG 3' Reverse 5' GGCCACTTTTCTCTTTCTTGG 3'
Doublesex (*dsx*)	AM 322 AM 323	Forward 5' CAGAGCATAGCACAGCACACGTC 3' Reverse 5' CCACTATTCGTGGGAGATGATGCC 3'
ApA Homeodomain CRISPR Guide	AM 158	5'GAAATTAATACGACTCACTATAGGAGCTGGTGATGCTT GAAGCGTTTTAGAGCTAGAAATAGC 3'
ApA LIM domain CRISPR guide	AM 235	5'GAAATTAATACGACTCACTATAGGAGAAACAGTGCACA TGAAACACGTTTTAGAGCTAGAAATAGC3'
ApB LIM domain CRISPR guide	AM 145	5'GAAATTAATACGACTCACTATAGGTGATGCGAGCCCGC GACAGTTTTAGAGCTAGAAATAGC3'
ApA Homeodomain Genotyping	AM 194 AM 167	Forward 5' CATTTTTGCGACACGAGACGTC 3' Reverse 5' CTAACTGTCTCGACTATATG 3'
ApA LIM domain CRISPR Genotyping	AM 257 AM 258	Forward 5' GTACAGTAATTAGTTCATCAAAC 3' Reverse 5' CTTTTCAGTTGTGTGCATTTTAAG 3'
ApB LIM domain CRISPR Genotyping	AM 385 AM 386	Forward 5' CACTAGATTAGCCTAAGGTC 3' Reverse 5' CTGTTTTGTAGGAGAAATATGG 3'

Table S2: CRISPR/Cas9 injection concentrations and mutation frequencies

Guide	Guide RNA Conc (ng/ul)	Cas9 mRNA Conc (ng/ul)	Number of eggs injected	Number of adults	Mutation Rate (%)+
ApA Homeodomain	360	600	631	9	44 (4/9)
	450	900	882	35	42.8 (15/35)*
ApA LIM Domain	400	900	424	17	47 (8/17)
ApB LIM Domain	400	900	228	45	26 (12/45)

+ The number within brackets is individuals with mutant wing phenotypes/total number of adults

* 4 of the 15 mutant individuals were pupae with wings missing from one side as shown in Figure 3F